New Class of Oligonuclear Platinum−Thallium Compounds with a Direct Metal-Metal Bond. 5. Structure Determination of Heterodimetallic Cyano Complexes in Aqueous Solution by EXAFS and Vibrational Spectroscopy

Farideh Jalilehvand,[†] Mikhail Maliarik,[†,‡] Magnus Sandström,*[,§] János Mink,[||,⊥] Ingmar Persson,[#] Per Persson,[&] Imre Tóth,[†,◇] and Julius Glaser*[,†]

Department of Chemistry, Inorganic Chemistry, Royal Institute of Technology (KTH), SE-100 44 Stockholm, Sweden, Department of Structural Chemistry, Arrhenius Laboratory, University of Stockholm, SE-106 91 Stockholm, Sweden, Department of Analytical Chemistry, University of Veszprém, P.O. Box 158, H-8201 Veszprém, Hungary, Institute of Isotope and Surface Chemistry of the Hungarian Academy of Sciences, P.O. Box 77, H-1525 Budapest, Hungary, Department of Chemistry, Swedish University of Agricultural Sciences, P.O. Box 7015, SE-750 07 Uppsala, Sweden, and Department of Chemistry, Inorganic Chemistry, Umeå University, SE-901 87 Umeå, Sweden

Received January 16, 2001

The structures of three closely related heterodimetallic cyano complexes, $[(NC)_5Pt-Tl(CN)_n]^{n-}$ ($n = 1-3$), formed in reactions between $[Pt^{II}(CN)_4]^{2-}$ and Tl^{III} cyano complexes, have been studied in aqueous solution. Multinuclear NMR data (^{205}Tl, ^{195}Pt, and ^{13}C) were used for identification and quantitative analysis. X-ray absorption spectra were recorded at the Pt and Tl L_{III} edges. The EXAFS data show, after developing a model describing the extensive multiple scattering within the linearly coordinated cyano ligands, short Pt−Tl bond distances in the $[(NC)_5Pt-Tl(CN)_n]^{n-}$ complexes: 2.60(1), 2.62(1), and 2.64(1) Å for $n = 1-3$, respectively. Thus, the Pt−Tl bond distance increases with increasing number of cyano ligands on the thallium atom. In all three complexes the thallium atom and five cyano ligands, with a mean Pt−C distance of 2.00−2.01 Å, octahedrally coordinate the platinum atom. In the hydrated $[(NC)_5Pt-Tl(CN)(H_2O)_4]^-$ species the thallium atom coordinates one cyano ligand, probably as a linear Pt−Tl−CN entity with a Tl−C bond distance of 2.13(1) Å, and possibly four loosely bound water molecules with a mean Tl−O bond distance of about 2.51 Å. In the $[(NC)_5Pt-Tl(CN)_2]^{2-}$ species, the thallium atom probably coordinates the cyano ligands trigonally with two Tl−C bond distances at 2.20(2) Å, and in $[(NC)_5Pt-Tl(CN)_3]^{3-}$ Tl coordinates tetrahedrally with three Tl−C distances at 2.22(2) Å. EXAFS data were reevaluated for previously studied mononuclear thallium(III)−cyano complexes in aqueous solution, $[Tl(CN)_2(H_2O)_4]^+$, $[Tl(CN)_3(H_2O)]$, and $[Tl(CN)_4]^-$, and also for the solid $K[Tl(CN)_4]$ compound. A comparison shows that the Tl−C bond distances are longer in the dinuclear complexes $[(NC)_5Pt-Tl(CN)_n]^{n-}$ ($n = 1-3$) for the same coordination number. Relative oxidation states of the metal atoms were estimated from their ^{195}Pt and ^{205}Tl chemical shifts, confirming that the $[(NC)_5Pt-Tl(CN)_n]^{n-}$ complexes can be considered as metastable intermediates in a two-electron-transfer redox reaction from platinum(II) to thallium(III). Vibrational spectra were recorded and force constants from normal-coordinate analyses are used for discussing the delocalized bonding in these species.

Introduction

Recently, it was found that a new family of heterometallic platinum−thallium cyano complexes, formed in reactions between $[Pt^{II}(CN)_4]^{2-}$ and thallium(III) cyano complexes, can exist in aqueous solution.[1,2] Multinuclear NMR spectroscopy, supported by Raman measurements,[2] showed that a direct metal−metal bond between the platinum and thallium atoms is present in the species. The number of cyano ligands in the complexes, at three different coordination sites, was also determined by means of multinuclear NMR spectroscopy. Structural models for the species were proposed, but neither the bond lengths, in particular the metal−metal distance, nor the hydration of the thallium atom was known.

The nature of the metal−metal bond in such heterometallic complexes is of interest in searching for reversible light-induced redox reactions, of potential use in, e.g., the conversion of light to chemical energy. The dinuclear complexes $[(NC)_5Pt-Tl(CN)_n]^{n-}$ ($n = 0-3$) can be regarded as metastable intermediates in a two-electron-transfer reaction between thallium(III) and platinum(II), leading to thallium(I) and platinum(IV) as final products. The complete redox reaction between these two metal

[†] Royal Institute of Technology (KTH).
[‡] Permanent address: Kurnakov Institute of General and Inorganic Chemistry, Russian Academy of Sciences, Leninsky Prospect 31, Moscow 117907, Russia.
[§] University of Stockholm.
[||] University of Veszprém.
[⊥] Institute of Isotope and Surface Chemistry of the Hungarian Academy of Sciences.
[#] Swedish University of Agricultural Sciences.
[&] Umeå University.
[◇] Permanent address: Department of Inorganic and Analytical Chemistry, University of Debrecen, H-4010 Debrecen, Pf. 21, Hungary.

(1) Berg, K. E.; Glaser, J.; Read, M. C.; Tóth, I. *J. Am. Chem. Soc.* **1995**, *117*, 7550.
(2) Maliarik, M.; Berg, K.; Glaser, J.; Sandström, M.; Tóth, I. *Inorg. Chem.* **1998**, *37*, 2910.

10.1021/ic010055h CCC: $20.00
Published on Web 06/27/2001

atoms can be induced by both optical and thermal pathways and results in cleavage of the metal−metal bond.[3,4]

A crystalline powder with the composition $TlPt(CN)_5$ can be precipitated from an aqueous solution of dimetallic Pt−Tl complexes.[2] Recently, its structure was studied by combining EXAFS, X-ray powder diffraction, and vibrational (IR/Raman) spectroscopy.[5] This allowed the unusual cyano-bridged structure of the compound to be established and the platinum−thallium bond length to be determined. In the present study, the EXAFS technique was applied to determine the metal−metal and metal−ligand bond distances of three dinuclear complexes, $[(NC)_5Pt-Tl(CN)_n]^{n-}$ ($n = 1-3$), in aqueous solution. This has become possible due to the developments in the data treatment implemented in the FEFF program, which in a simple way allows selection of the important pathways for modeling the excessive multiple scattering of the linearly coordinated cyano ligands.[6,7] Normal-coordinate analyses of vibrational spectra, together with NMR results, allowed comparisons of the structure and bond character in these complexes.

Experimental Section

Materials and Syntheses. All starting materials and preparative routes used to obtain the studied complexes, $[(NC)_5Pt-Tl(CN)_n]^{n-}$, in aqueous solution have been described previously.[2] The concentrations (mol dm^{-3}) of the dominating dimetallic complexes and their percentages (in parentheses) of the total amounts of the dimetallic Pt−Tl complexes in each solution were 0.075 (95%), 0.050 (75%), and 0.056 (95%) for the $[(NC)_5Pt-Tl(CN)(H_2O)_4]^-$, $[(NC)_5Pt-Tl(CN)_2]^{2-}$, and $[(NC)_5Pt-Tl(CN)_3]^{3-}$ solutions, respectively. In the $[(NC)_5Pt-Tl(CN)_3]^{3-}$ solution, also unreacted mononuclear $[Pt(CN)_4]^{2-}$ and $[Tl(CN)_4]^-$ complexes remain, about 0.014 mol dm^{-3} each. The distribution of the complexes has been determined by NMR methods.[8] The analysis of the concentration of free acid, thallium(III), and thallium(I) in aqueous solution has been described previously.[9]

Methods and Measurements. NMR Measurements. All NMR spectra of the solutions were recorded with a Bruker AM400 spectrometer at a probe temperature of 298 (±0.5) K. Detailed information on typical NMR parameters for obtaining ^{205}Tl, ^{195}Pt, and ^{13}C spectra have been given in recent publications from this laboratory.[1,2]

Vibrational Spectroscopy. Raman spectra of the solutions were measured by means of a Bio-RAD FTS 6000 FT-IR spectrometer equipped with an FT-Raman accessory. The 1064 nm line from a Spectra-Physics Nd:YAG laser was used to irradiate the samples contained in 5 mm NMR tubes with about 1200 mW, and 2000 scans were collected at a spectral bandwidth of 4 cm^{-1}. The infrared absorption (IR) spectra in the cyanide C−N stretching region of the aqueous solutions were recorded by means of a Bio-RAD FTS 375 spectrometer, using a CaF_2 windowed cell and 25 μm Teflon spacers. In our previous paper,[2] a Raman band which appeared at 2210 cm^{-1} was ascribed to the apical cyano ligand of the $[(NC)_5Pt-Tl(CN)_n]^{n-}$ complexes. However, it was later found to originate from $[Pt(CN)_6]^{2-}$ species,[19,24] formed as a result of a partial redox photodecomposition when the complexes were irradiated with high-energy 514.5 nm laser radiation from an argon ion laser. With the 1064 nm infrared laser line used in the present work, no C−N band was observed at frequencies higher than 2200 cm^{-1} for the dimetallic complexes in solution (cf. Figure 4b).

EXAFS Measurements. Pt and Tl L_{III}-edge EXAFS data were collected in transmission mode (in one case also in fluorescence mode using a Lytle detector) at beamline 4-1 at the Stanford Synchrotron Radiation Laboratory (SSRL). The experimental conditions were similar to those described previously.[10] The energy calibration was made with a simultaneously measured transmission spectrum of a platinum or thallium foil with the first inflection point set to 11 564 and 12 658 eV, respectively. For these dimetallic samples the usable range of the Pt L_{III} edge EXAFS data is limited to $k < 15$ $Å^{-1}$ by the Tl L_{III} edge, and that of the Tl L_{III} range is limited to $k < 12$ $Å^{-1}$ by the Pt L_{II} edge at 13 273 eV. Typically, three to four scans were averaged for each sample. Solution cells with polypropylene foil (~6 μm) or thin glass (~35 μm) windows, and Vitone or Teflon spacers (3−5 mm), were used. No useful EXAFS data could be obtained for the $[(NC)_5Pt-Tl(H_2O)_x]$ complex in solution, due to its low solubility and rapid redox decomposition in the intense synchrotron X-ray beam.

EXAFS Data Treatment. The EXAFS data were energy-calibrated and averaged by means of the EXAFSPAK program.[11] The remaining data treatment, including standard procedures for preedge subtraction, data normalization, and spline removal, was made using the WinXAS program.[12] The k^3-weighted EXAFS oscillations were Fourier-transformed over the k range 2.6−15 $Å^{-1}$ for the Pt data and 3−12 $Å^{-1}$ for Tl, using a Bessel window function. After Fourier filtering, the k^3-weighted EXAFS functions were used for model fitting by least-squares refinements of the model parameters. The theoretical phase and amplitude functions for single and multiple scattering within the assumed molecular model were calculated using ab initio methods by means of the FEFF7 program code.[6]

The estimated standard deviations s for the refined parameters given in the tables are obtained from the noise level at high k of the zero-weighted EXAFS function $\chi(k)$ and do not include systematic errors of the measurements. However, the variations in the refined parameters, including the shift in the E_0 value (for which $k = 0$), using different models and data ranges, indicate that the accuracy of the absolute values of the distances given for the separate complexes is within ±0.02 Å.

EXAFS Models. The EXAFS data analysis of the Pt L_{III}-edge data is complicated by the very intense multiple scattering originating from the almost linearly coordinated cyanide groups. All Fourier transforms display two prominent peaks, the first of which corresponds to the Pt−C single-scattering path, as shown by the spectra for the standard compounds $K_2[Pt^{II}(CN)_4]\cdot 3H_2O$ and $K_2[Pt^{IV}(CN)_6]$ (Figures S1 and S2; Supporting Information). The second peak, however, is much larger than that calculated for single Pt−N backscattering. According to the FEFF calculations (performed assuming stationary atoms), this peak is dominated by several strong multiple-scattering contributions. This is also evident from the similarity between the EXAFS spectra of the three solution complexes $[(NC)_5Pt-Tl(CN)_n]^{n-}$ ($n = 1-3$) and the spectra of the solid compounds $K_2[Pt^{II}(CN)_4]\cdot 3H_2O$ and $K_2[Pt^{IV}(CN)_6]$ (cf. Figure 1 and Figures S1 and S2). The contribution from the Pt−Tl interaction is largely obscured in the Fourier transform by these overlapping interactions. Thus, to obtain reliable values of the Pt−Tl distance, one of the main purposes of this study, it was necessary to develop a model that accounts for both the single- and multiple-scattering contributions from the linear Pt−C−N entities.

The amplitude of the EXAFS function is directly proportional to both the frequency of the distances and the amplitude reduction factor, S_0^2. Therefore, the known coordination numbers were used for the model compounds in order to obtain experimental S_0^2 values by least-squares refinements. The S_0^2 values determined in this way are somewhat higher than expected (theoretically about 0.8−0.9; cf. Tables S1−S3 in the Supporting Information). One reason could be that fluorescence

(3) Maliarik, M.; Glaser, J.; Tóth, I. *Inorg. Chem.* **1998**, *37*, 5452.
(4) Khoshtariya, D. E.; Maliarik, M.; Tóth, I.; Glaser, J. Submitted for publication.
(5) Jalilehvand, F.; Eriksson, L.; Glaser, J.; Maliarik, M.; Mink, J.; Sandström, M.; Tóth, I.; Tóth, J. *Chem. Eur. J.*, in press.
(6) Zabinsky, S. I.; Rehr, J. J.; Ankudinov, A.; Albers, R. C.; Eller, M. J. *Phys. Rev. B* **1995**, *52*, 2995. Ankudinov, A. L.; Rehr, J. J. *Phys. Rev. B* **1997**, *56*, R1712. The FEFF program is available at http://Feff.phys.washington.edu/feff.
(7) Rehr, J. J.; Ankudinov, A.; Zabinsky, S. I. *Catal. Today* **1998**, *39*, 263.
(8) Maliarik, M.; Glaser, J.; Tóth, I.; W. da Silva, M.; Zekany, L. *Eur. J. Inorg. Chem.* **1998**, 565.
(9) Blixt, J.; Györi, B.; Glaser, J. *J. Am. Chem. Soc.* **1989**, *111*, 7784.
(10) Blixt, J.; Glaser, J.; Mink, J.; Persson, I.; Persson, P.; Sandström, M. *J. Am. Chem. Soc.* **1995**, *117*, 5089.
(11) George, G. N.; Pickering, I. J. In *EXAFSPAK−A Suite of Computer Programs for Analysis of X-ray Absorption Spectra*; George, G. N., Pickering, I. J., Eds.; SSRL: Stanford, CA, 1993.
(12) Ressler, T. *J. Synchrotron Radiat.* **1998**, *5*, 118.

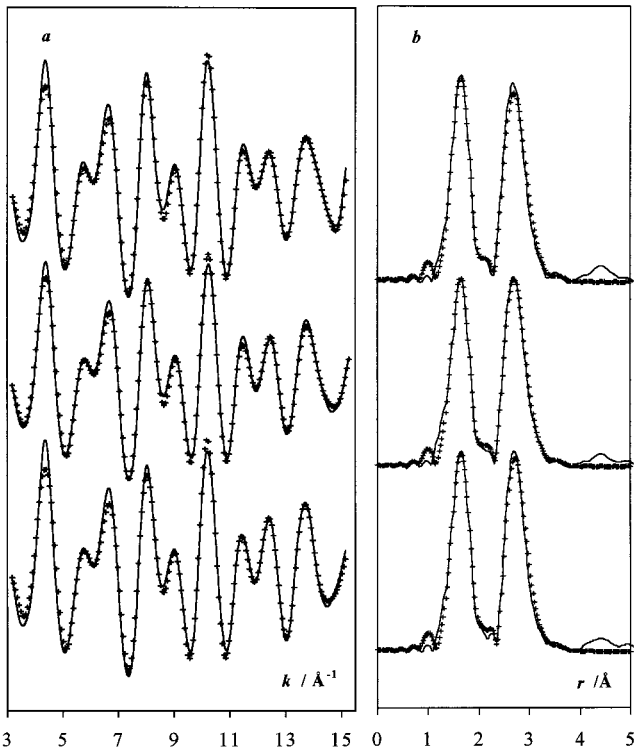

Figure 1. Pt L_{III}-edge EXAFS, k^3-weighted and Fourier filtered (1.1−8 Å), of aqueous solutions with the dominating species $[(NC)_5Pt-Tl(CN)_n]^{n-}$ (n = 1−3) from top to bottom, respectively: (a) experimental (solid lines) and model EXAFS functions; (b) Fourier transforms.

Scheme 1. Main EXAFS Scattering Pathways in the Linear M−C−N Units (M = Pt, Tl)[a]

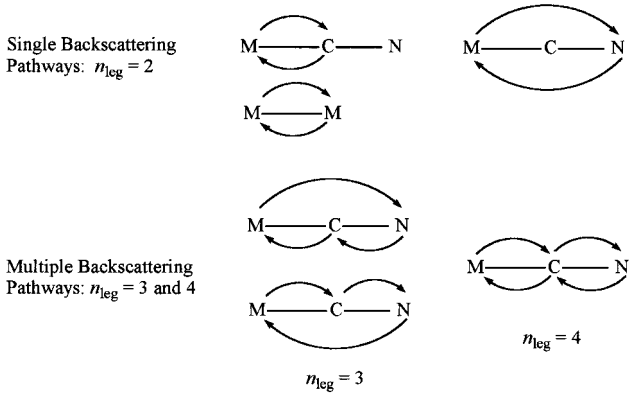

[a] There are two degenerate three-legged scattering pathways M−C−N (n_{leg} = 3).

radiation from the sample adds to the signal monitored in the I_0 ion chamber before the sample and thereby causes an apparent increase in the amplitude of the transmitted EXAFS, another reason could be that for L_{III} edges the S_0^2 values sometimes tend to be higher than 1.0, when using simplified multiple scattering models based on the FEFF program (see below).

The compounds $K_2[Pt^{II}(CN)_4]\cdot 3H_2O$ and $K_2[Pt^{IV}(CN)_6]$, with known structures,[13,14] were used to test such models. We found that their EXAFS spectra could be satisfactorily described with a model comprising Pt−C and Pt−N backscattering (n_{leg} = 2), together with linear three-legged (n_{leg} = 3) Pt−C−N and four-legged (n_{leg} = 4) Pt−C−N−C multiple scattering pathways (Scheme 1). The two degenerate three-legged Pt−C−N scattering pathways give the dominating contribution

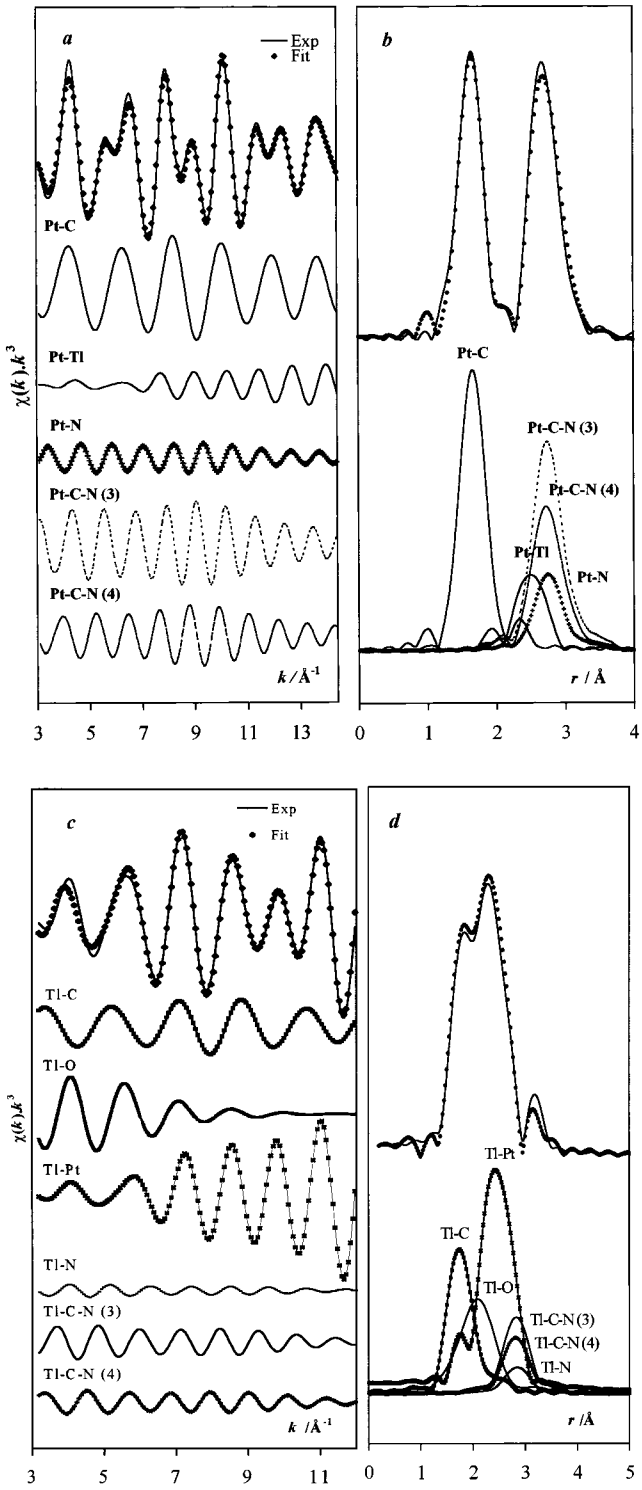

Figure 2. k^3-weighted and Fourier-filtered EXAFS of the $[(NC)_5Pt-Tl(CN)(H_2O)_4]^-$ species, (top solid line, experimental; dots, model) with individual model contributions (a) below the Pt L_{III} edge with (b) corresponding Fourier transforms (c) below the Tl L_{III} edge with (d) Fourier transforms.

to the EXAFS spectrum (Figure 2a,b and Figures S1a and S2a in the Supporting Information). Therefore, the refined Pt−N distance and Debye−Waller factor of this pathway were used as the principal parameters also in the description of the other scattering pathways involving the nitrogen atom. The use of the same σ^2 value for all three paths (Table 1) can be justified by the "independent vibration approximation" model.[15] The results of the refinements are given in Table S1 (Supporting Information) for the standard compounds, and the distances obtained by means of this multiple-scattering model are

(13) Washecheck, D. M.; Peterson, S. W.; Reis, A. H.; Williams, J. M. *Inorg. Chem.* **1976**, *15*, 74.
(14) Weiss, J. *Z. Naturforsch.* **1974**, *29B*, 119.

Table 1. Pt L_{III} EXAFS Results of Model Refinements for Dimetallic Cyano Complexes in Solution:[a] Backscattering Pathways n_{leg},[b] Interatomic Distances *d*, and Mean Square Deviations (Debye−Waller Parameter) σ^2

main complex in soln	n_{leg}	freq of pathway	*d*/Å	σ^2/Å^2
$[(NC)_5Pt-Tl(CN)(H_2O)_4]^-$	Pt−C	5	2.009(2)	0.0027(1)
	Pt−Tl	1	2.602(2)	0.0049(2)
	Pt−N	5	3.162	0.0047
	Pt−C−N (3)	10	3.162(2)	0.0047(2)
	Pt−C−N (4)	5	3.162	0.0047
$[(NC)_5Pt-Tl(CN)_2]^{2-}$	Pt−C	5	2.003(2)	0.0032(1)
	Pt−Tl	1	2.613(3)	0.0055(3)
	Pt−N	5	3.151	0.0049
	Pt−C−N (3)	10	3.151(2)	0.0049(2)
	Pt−C−N (4)	5	3.151	0.0049
$[(NC)_5Pt-Tl(CN)_3]^{3-}$	Pt−C	5	2.008(2)	0.0029(1)
	Pt−Tl	1	2.637(4)	0.0055(3)
	Pt−N	5	3.162	0.0048
	Pt−C−N (3)	10	3.162(2)	0.0048(2)
	Pt−C−N (4)	5	3.162	0.0048

[a] k^3-weighted Fourier-filtered data. For independently refined model parameters, estimated standard deviations are given in parentheses. The distance *d* and Debye−Waller parameter σ for Pt−N and Pt−C−N ($n_{leg} = 4$) are correlated to the dominant multiple scattering pathway Pt−C−N ($n_{leg} = 3$). [b] See Scheme 1.

in excellent agreement with the mean crystallographic values (in parentheses): Pt−C = 1.985 (1.989) Å and Pt−N = 3.149 (3.148) Å for $K_2[Pt(CN)_4]\cdot 3H_2O$,[13] Pt−C = 2.004 (2.005) Å and Pt−N = 3.155 (3.153) Å for $K_2[Pt(CN)_6]$.[14]

The unfiltered data for the standard compound $K_2[Pt(CN)_4]\cdot 3H_2O$ were also modeled using the GNXAS method,[16] including contributions from several additional four-legged minor multiple-scattering pathways.[17] This gave bond distances in excellent agreement with those above (Pt−C = 1.987 Å, Pt−N = 3.146 Å). Even though the amplitude reduction factor became lower, $S_0^2 = 0.91$, this shows that the distances obtained are independent of the program system used.

Essentially the same FEFF-based model, including multiple scattering according to Scheme 1, could also be used to describe the Tl L_{III} EXAFS oscillations (Figure 2c) from the linearly coordinated Tl−C−N entities in the complexes $[(NC)_5Pt-Tl(CN)_n]^{n-}$ ($n = 1-3$) (Tables 2 and S2). In this case there are pronounced differences between the Tl L_{III} spectra (Figure 3), resulting from the different number of cyano ligands and coordination environments of the thallium atom in the $-Tl(CN)_n$ entities.

In addition, the same multiple-scattering model was successfully applied in this work on the previously collected data for the mononuclear $[Tl(CN)_{n+1}]^{3-(n+1)}$ complexes in aqueous solution[10] and for the solid compound $K[Tl(CN)_4]$ (Table 2 and Table S3 (Supporting Information)). Previously, the same model was used for the solid $TlPt(CN)_5$ (Tables S1 and S2).[5] The reason the same model can be used also for the solid compounds is because the effective multiple-scattering contributions are completely dominated by the local short-range resonances within the linearly coordinated ligands. Very recently, a similar multiple-scattering treatment was published for the planar $[Ni(CN)_4]^{2-}$ complex, confirming this conclusion.[18] By means of FEFF calculations, different cluster sizes for the $K_2[Ni(CN)_4]$ structure were used to reproduce features in the near-edge region. Also in the EXAFS region additional multiple scattering pathways, including correlation between the Debye−Waller factors, were tested. The conclusion was that exactly the same type of model as the one used here was sufficient for analyzing these $[Ni(CN)_4]^{2-}$ X-ray absorption data, both from solution and from the solid compound.

Table 2. Tl L_{III} EXAFS Results of Model Refinements for Cyano Complexes in Solution and for Solid $K[Tl(CN)_4]$:[a] Backscattering Pathway n_{leg}, Interatomic Distances *d*, Mean Square Deviations (Debye−Waller Parameter) σ^2

main complex in soln	n_{leg}	freq of pathway	*d*/Å	σ^2/Å^2
$[(NC)_5Pt-Tl(CN)(H_2O)_4]^-$	Tl−C	1	2.128(6)	0.0027(3)
	Tl−O	4	2.505(5)	0.023(1)
	Tl−Pt	1	2.595(1)	0.0030(1)
	Tl−N	1	3.284	0.0091
	Tl−C−N (3)	2	3.284(6)	0.0091(8)
	Tl−C−N (4)	1	3.284	0.0091
$[(NC)_5Pt-Tl(CN)_2]^{2-}$	Tl−C[b]	2	2.206(6)	0.0051(6)
	Tl−Pt	1	2.622(3)	0.0064(6)
	Tl−N	2	3.356	0.0073
	Tl−C−N (3)	4	3.356(3)	0.0073(6)
	Tl−C−N (4)	2	3.356	0.0073
$[(NC)_5Pt-Tl(CN)_3]^{3-}$	Tl−C[c]	3	2.203(6)	0.0069(5)
	Tl−Pt	1	2.639(8)	0.009(1)
	Tl−N	3	3.355	0.0100
	Tl−C−N (3)	6	3.355(5)	0.0100(7)
	Tl−C−N (4)	3	3.355	0.0100
$[Tl(CN)_2(H_2O_2)_4]^+$	Tl−C	2	2.092(4)	0.0029(3)
	Tl−O	4	2.429(4)	0.0029(3)
	Tl−N	2	3.263	0.0055
	Tl−C−N (3)	4	3.263(3)	0.0055(3)
	Tl−C−N (4)	2	3.263	0.0055
$[Tl(CN)_3(H_2O_2)]$	Tl−C	3	2.133(4)	0.0039(3)
	Tl−O	1	2.42(2)	0.0089(23)
	Tl−N	3	3.293	0.0056
	Tl−C−N (3)	6	3.293(3)	0.0056(3)
	Tl−C−N (4)	3	3.293	0.0056
$[Tl(CN)_4]^-$	Tl−C	4	2.176(6)	0.0042(4)
	Tl−N	4	3.322	0.0060
	Tl−C−N (3)	8	3.322(5)	0.0060(6)
	Tl−C−N (4)	4	3.322	0.0060
$K[Tl(CN)_4]_s$	Tl−C	4	2.172(5)	0.0043(3)
	Tl−N	4	3.323	0.0060
	Tl−C−N (3)	8	3.323(4)	0.0060(4)
	Tl−C−N (4)	4	3.323	0.0060

[a] k^3-weighted Fourier-filtered data. For independently refined model parameters, estimated standard deviations are given in parentheses. The distance *d* and Debye−Waller parameter σ for Tl−N and Tl−C−N ($n_{leg} = 4$; cf. Scheme 1) are correlated to the dominant multiple-scattering pathway Tl−C−N ($n_{leg} = 3$). [b] Estimated to Tl−C = 2.20(2) Å when corrected for influence of minor complexes; see text. [c] Estimated to Tl−C = 2.22(2) Å when corrected for influence of 25% $[Tl(CN)_4]^-$; see text.

Analyses of Vibrational Spectra. Raman and IR spectra are shown in Figure 4, and the experimentally obtained fundamental frequencies of the three complexes $[(NC)_5Pt-Tl(CN)_n]^{n-}$ ($n = 1-3$) are listed in Table 3. A common problem for vibrational spectroscopy from aqueous solutions is the low resolution of the observed spectra. For the previously studied closely related complex $[(NC)_5PtI]^{2-}$, with 21 Raman active fundamentals, only 7 Raman bands could be observed.[19] A similar situation occurs in the present case, with e.g. 8 recorded bands out of 24 possible Raman-active modes of the $[(NC)_5Pt-Tl(CN)]^-$ complex (Table 3). This is due to the broad and strongly overlapping bands and the difficulty in obtaining low-frequency spectra (below 120 cm^{-1}) in aqueous media. In addition, for transmission IR spectra the strong absorption by the bulk water obscures the solute spectra in some regions. Even though curve-fitting methods were used to analyze the spectra, the only way to solve the assignment problem for those fundamentals which are close in energy, giving unresolved frequencies within a broad band in the spectrum, is to assign them all to the same experimental frequency (see Appendix and Table S4, Supporting Information).

(15) Yokoyama, T.; Kobayashi, K.; Ohta, T.; Ugawa, A. *Phys. Rev. B* **1996**, *53*, 6111.
(16) Filliponi, A.; DiCicco, A.; Natoli, C. R. *Phys. Rev. B.* **1995**, *52*, 15122 and references therein. GNXAS software package for EXAFS data analysis, available at http://www.aquila.infn.it/gnxas/.
(17) Jalilehvand, F.; Persson, I.; Sandström, M.; Stålhandske, C. M. V. Unpublished results.
(18) Muños-Páez, A.; Díaz-Moreno, S.; Sánchez Marcos, E.; Rehr, J. J. *Inorg. Chem.* **2000**, *39*, 3784.
(19) Memering, M. N.; Jones, L. H.; Bailar, J. C. *Inorg. Chem.* **1973**, *12*, 2793.

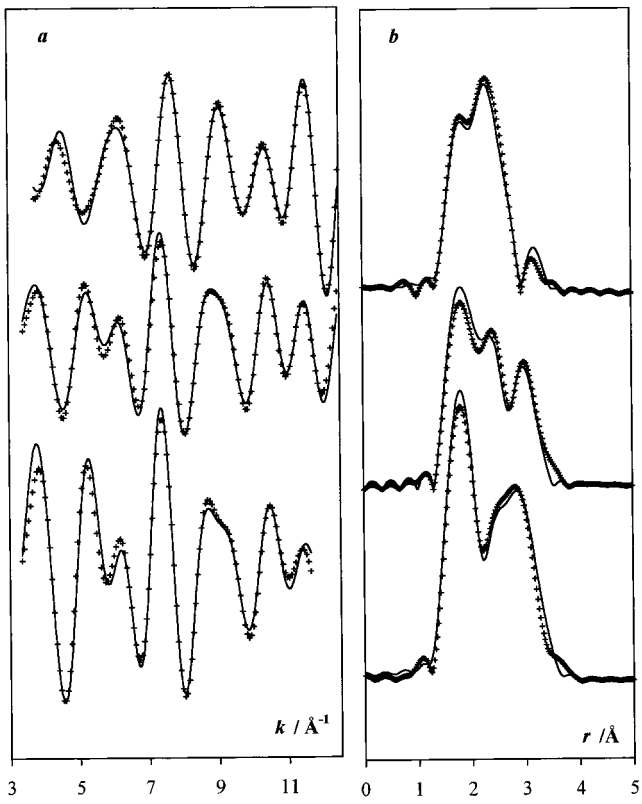

Figure 3. Tl L_{III} EXAFS, k^3-weighted and Fourier filtered (1.4−3.5 Å), of aqueous solutions with the dominating species $[(NC)_5Pt-Tl(CN)_n]^{n-}$ ($n = 1-3$) from top to bottom, respectively: (a) experimental (solid lines) and model EXAFS functions; (b) Fourier transforms.

A simplified description of the vibrational spectra of the present solution species is therefore necessary in order to allow normal-coordinate analyses. The complex $[(NC)_5Pt-Tl(CN)]^-$ can be described in C_{4v} symmetry, and the complex $[(NC)_5Pt-Tl(CN_2)]^{2-}$ probably belongs to the C_{2v} point group and $[(NC)_5Pt-Tl(CN_3)]^{3-}$ to C_s. However, the last two complexes can be satisfactorily characterized by using the local symmetries of the Pt and Tl fragments. For the analyses, the dimetallic complexes can be divided into a common part, which is the $(NC)_5Pt-$ group with local C_{4v} symmetry, and a $-Tl(CN)_n$ group with local C_{2v} symmetry for $-Tl(CN)_2$ and C_{3v} for $-Tl(CN)_3$. Assignments according to these local symmetries are reported in Table S4 (Supporting Information) and are based on calculated frequencies and comparisons with previous assignments of related complexes.[10,19] A detailed discussion of the proposed assignment and possible alternatives is given in an Appendix in the Supporting Information.

Wilson's **GF** matrix method was used for the calculation of vibrational frequencies using a symmetrized valence force field. The initial force constants were adopted from Jones et al.[19−22] and from Blixt et al.[10] and refined to give a satisfactory fit of calculated to experimental frequencies by means of a PC-based program package.[23] The internal coordinates are illustrated in Figure S3 (Supporting Information). The fundamental modes, their potential energy distributions over the internal coordinates, and force constants for the best fit are given in Tables S4 and S5 (Supporting Information). For a consistency check, the $[Pt(CN)_6]^{2-}$ complex was reevaluated from literature data, with results in satisfactory agreement with the previous investigation.[24]

(20) Jones, L. H.; Smith, J. M. *Inorg. Chem.* **1965**, *4*, 1677.
(21) Jones, L. H. *Inorganic Vibrational Spectroscopy*; Marcel Dekker: New York, 1971.
(22) Kubas, G. J.; Jones, L. H. *Inorg. Chem.* **1974**, *13*, 2816.
(23) Mink, J.; Mink, L. M. *Computer Program System for Vibrational Analyses of Polyatomic Molecules*; Mink, J., Mink, L. M., Eds.; Department of Analytical Chemistry, Veszprém University: P.O. Box 158, H-8201 Veszprém, Hungary.
(24) Siebert, H.; Siebert, A. *Z. Naturforsch.* **1967**, *22B*, 674.

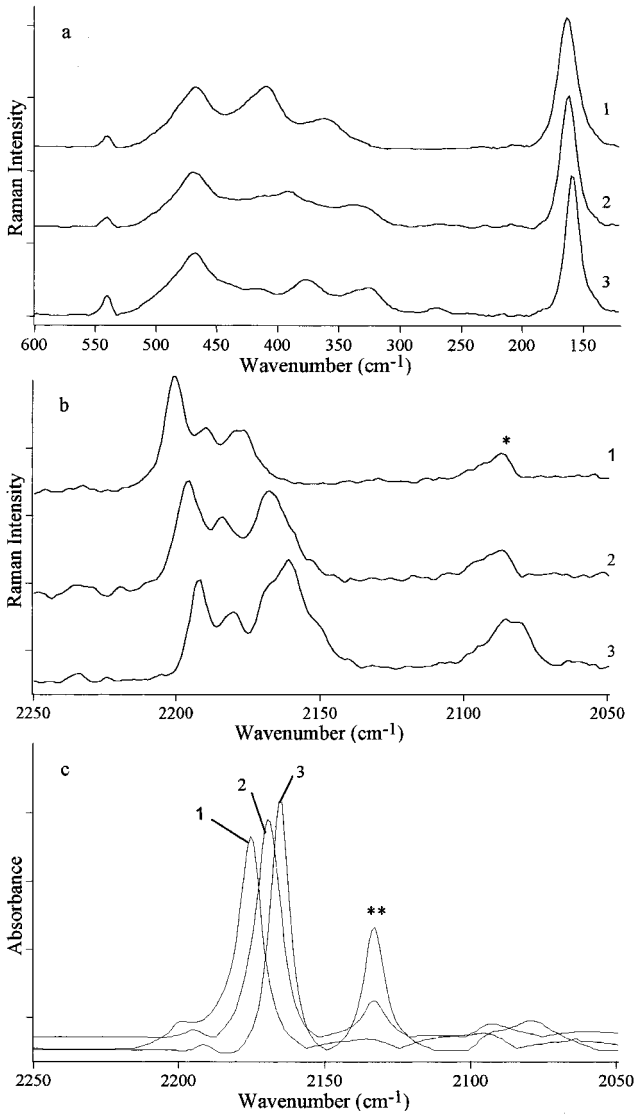

Figure 4. Vibrational spectra of the dimetallic complexes $[(NC)_5Pt-Tl(CN)_n]^{n-}$ ($n = 1-3$) in aqueous solution: (a) Raman low-frequency region (smoothed, base-line corrected); (b) Raman C−N stretching region (interpolated); (c) IR absorption (baseline corrected) C−N region (* free CN^- ion, ** E_u band of $[Pt(CN)_4]^{2-}$).

Results and Discussion

Structure of the Complexes in Aqueous Solution. Multinuclear NMR spectroscopy showed that three different types of cyano ligands are present in the dinuclear Pt−Tl bonded $[(NC)_5Pt-Tl(CN)_n]^{n-}$ ($n = 0-3$) complexes.[2] The platinum atom is coordinated by four equivalent cyano ligands, and the same square-planar coordination geometry is assumed to prevail as in the starting $[Pt(CN)_4]^{2-}$ complex. A fifth axial cyano ligand, in a position trans to the platinum−thallium bond, completes an octahedral six-coordination around platinum with a similar pentacyanoplatinum entity in all four complexes.

The results of the Pt and Tl L_{III}-edge EXAFS analyses carried out for the aqueous solutions of the complexes $[(NC)_5Pt-Tl(CN)_n]^{n-}$ ($n = 1-3$) are fully in agreement with the previous spectroscopic findings. A nonbuttressed Pt−Tl bond directly links the pentacyanoplatinum unit to the thallium cyano group. The length of the metal−metal bond and the coordination environment of the metal atoms in the complexes are discussed in detail below. The Pt and Tl L_{III}-edge EXAFS data for the complexes are summarized in Tables 1 and 2, and the EXAFS

Table 3. Vibrational Fundamental Frequencies (cm^{-1}) from Raman and IR Spectra of the Dimetallic Cyano Complexes in Aqueous Solution[a]

$[(NC)_5PtTl(CN)]^-$		$[(NC)_5PtTl(CN)_2]^{2-}$		$[(NC)_5PtTl(CN)_3]^{3-}$		
Raman	IR	Raman	IR	Raman	IR	approx assign[a]
2200.1 vs, p	2199.5 m	2195.6 vs, p	2196 s	2191.8 vs,p	2192 w	CN str (eq)
2189.8 s, m		2183.3 m		2180.5 m		CN str (eq)
	2175.4 s		2169.4 s		2165.5 s	CN str (eq)
2177.6 s, br		2167.8 s, br		2160.5 vs		CN str (ax)
2177.6 s, br		2167.8 s, br		2160.5 vs		CN str (Tl)
			2169.4 s		2165.5 s	CN str (Tl)
468 m		468 m		467.7 m		PtC str (eq), PtCN def (eq)
				439 w		PtCN def (eq)
411 m		414 vw		415 w		PtC str (eq), PtC str (ax), PtCN def (eq), PtCN def (ax)
362 w		333 w		376 m		TlC sym str
		392 w		328.8 w		TlC asym str
260 vw		267 w		269.8 w		TlCN def
163.7 vs		162.6 vs		159.1 vs		PtTl str

[a] Abbreviations: br, broad; m, medium; p, polarized; s, strong; vs, very strong; w, weak; vw, very weak; eq, equatorial; ax, axial; str, stretch; sym, symmetrical; def, deformation. The symmetry species are not specified, because of overlapping bands belonging to several irreducible representations (cf. Table S4).

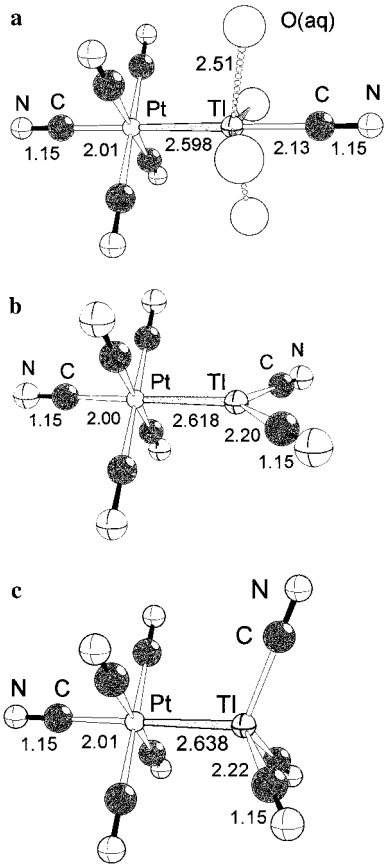

Figure 5. Structural models proposed for the dimetallic complexes in aqueous solution (distances in Å): (a) $[(NC)_5Pt-Tl(CN)(H_2O)_4]^-$; (b) $[(NC)_5Pt-Tl(CN)_2]^{2-}$; (c) $[(NC)_5Pt-Tl(CN)_3]^{3-}$.

fits and Fourier transforms are shown in Figures 1−3. Proposed structural models for the complexes consistent with these results are shown in Figure 5.

Further details of the analyses of the EXAFS data are given in Tables S1−S3, and assignments and treatment of the vibrational spectra are discussed in the Supporting Information. Results of the normal coordinate analyses are given in Tables 4 and 5 and in Tables S4 and S5 (Supporting Information).

Characterization of the Metal−Metal Bond. For the $[(NC)_5Pt-Tl(CN)(H_2O)_4]^-$ complex the Fourier transform of the Pt−Tl contribution to the EXAFS spectra of the Pt and Tl atoms is shown separately in parts b and d of Figure 2. The overlap with the strong multiple-scattering features, Pt−C−N

Table 4. Comparison of C−N and M−C Stretching Force Constants (N cm^{-1}) for Platinum(IV) and Thallium(III) Cyano Complexes

complex	*K*(CN)	*K*(MC)	ref
$[Pt(CN)_6]^{2-}$	17.43	2.94	this work, 24[c]
$[Pt(CN)_5Cl]^{2-}$	17.62,[a] 17.80[b]	2.89,[a] 2.92[b]	this work, 19[c]
$[Pt(CN)_5Br]^{2-}$	17.57,[a] 17.65[b]	2.90,[a] 2.85[b]	this work, 19[c]
$[Pt(CN)_5I]^{2-}$	17.48,[a] 17.49[b]	2.88,[a] 2.72[b]	this work, 19[c]
$[(NC)_5\mathbf{Pt}Tl(CN)]^-$	17.36,[a] 17.36[b]	2.76,[a] 2.38[b]	this work
$[(NC)_5\mathbf{Pt}Tl(CN)_2]^{2-}$	17.30,[a] 17.22[b]	2.82,[a] 2.40[b]	this work
$[(NC)_5\mathbf{Pt}Tl(CN)_3]^{3-}$	17.18,[a] 17.19[b]	2.81,[a] 2.43[b]	this work
$[Pt(CN)_4Cl_2]^-$	17.30	2.79	20
$[Pt(CN)_4Br_2]^-$	17.23	2.81	20
$[Pt(CN)_4I_2]^-$	17.06	2.78	20
$[Pt(CN)_4]^{2-}$	17.41	2.75	22
$[TlCN]^{2+}$	17.73	2.36	10
$[Tl(CN)_2]^+$	17.62	2.34	10
$[Tl(CN)_3]$	17.60	2.13	10
$[Tl(CN)_4]^-$	17.56	1.80	10
$[(NC)_5Pt\mathbf{Tl}CN]^-$	17.50[d]	1.89[d]	this work
$[(NC)_5Pt\mathbf{Tl}(CN)_2]^{2-}$	17.23[d]	1.81[d]	this work
$[(NC)_5Pt\mathbf{Tl}(CN)_3]^{3-}$	17.39[d]	1.66[d]	this work

[a] Four equatorial cyano ligands in $(NC)_5\mathbf{Pt}-$ group. [b] Axial cyano ligand of platinum. [c] Experimental frequencies taken from this reference. [d] Cyano ligands in $-\mathbf{Tl}(CN)_n$ group.

($n_{leg} = 3$) and Pt−C−N ($n_{leg} = 4$), shows why the contribution from the Pt−Tl bond is difficult to detect in the Pt L_{III} edge EXAFS data and explains the similarity of the EXAFS oscillations in Figure 1. In the Tl L_{III} edge spectra, however, the Pt−Tl bond makes a major contribution, particularly at high *k* values (Figure 2c). Even though the cyano ligands are more strongly dominating in the Tl L_{III}-edge spectra for the $[(NC)_5Pt-Tl(CN)_2]^{2-}$ and $[(NC)_5Pt-Tl(CN)_3]^{3-}$ solutions, the Pt−Tl contribution is still discernible in the Fourier transform for all three solutions (Figure 3). However, in the EXAFS functions the oscillating contribution from the platinum−thallium interaction has an increasing envelope at high *k* values, which distinguishes it from other scattering paths. Therefore, in the model refinements the Pt−Tl bond distance could be obtained independently from both the Pt and the Tl L_{III}-edge EXAFS, with high precision and in satisfactory agreement for the same solution (Tables 1 and 2).

The weighted average Pt−Tl bond distances for the $[(NC)_5Pt-Tl(CN)_n]^{n-}$ ($n = 1-3$) complexes are given in Table 5 (2.60(1), 2.62(1), and 2.64(1) Å, respectively) and include estimated uncertainties from systematic errors in the data and the distribution of complexes in the solutions. Thus, the increasing number of cyano ligands results in a smooth increase in the metal−

Table 5. Characteristics of the Pt−Tl Bond in the Dinuclear Complexes in Aqueous Solution

complex	d_{Pt-Tl}, Å	$^1J(^{195}Pt-^{205}Tl)$, Hz	ν(Pt−Tl), cm^{-1}	K(PtTl),[a] N cm^{-1}	δ_{Pt}, ppm[b]	Pt "rel oxidn state"	δ_{Tl}, ppm[b]	Tl "rel oxidn state"
$Pt^{IV}(CN)_6^{2-}$					655	+4		
Tl^{I}							0	+1
$[(NC)_5Pt-Tl(H_2O)_x]$		71 060			474	+3.6 (+3.2)[c]	786	+1.5 (+1.6)[c]
$[(NC)_5Pt-Tl(CN)(H_2O)_4]^-$	2.60(1)	57 020	163.7	1.736	383	+3.4	1371	+1.9
$[(NC)_5Pt-Tl(CN)_2]^{2-}$	2.62(1)	47 260	162.6	1.693	184	+2.9	1975	+2.3
$[(NC)_5Pt-Tl(CN)_3]^{3-}$	2.64(1)	38 760	159.1	1.563	68	+2.6	2224	+2.5
$Tl^{III}(CN)_4^-$							3010	+3
$Pt^{II}(CN)_4^{2-}$					−213	+2		

[a] Full normal-coordinate analysis including all atoms in the complex. [b] From ref 2. [c] Numbers in parentheses were determined by means of X-ray photoelectron spectroscopy (XPS) for the solid $[(NC)_5PtTl]$.[5]

metal bond distance. For all three compounds these short distances unambiguously demonstrate formation of a direct Pt−Tl bond and confirm the conclusions from our previous spectroscopic studies.[1,2]

The stretching vibration of the Pt−Tl bond, which appears as an intense polarized Raman band, occurs at low wavenumbers due to the large masses of the two bound atoms (Figure 4).[2] The vibration frequency decreases as expected with increasing Pt−Tl bond length but is not very sensitive to the change in the metal−metal distance (Table 5). To compare the overall strength of the Pt−Tl bond in the compounds, force constants of the metal−metal bond stretch were calculated using different approximations in the normal-coordinate analyses, from considering only the metal atoms to including the full cyano coordination around the metal atoms. The values obtained for the Pt−Tl stretching force constants are characteristic for single metal−metal bonds[25,26] but differ by as much as about 20% for different approximations in the models (Figure 6). The decrease in the force constant with increasing bond distance is more clear-cut than the relatively small decrease in the vibrational frequency, which is partly due to a compensating effect from the increasing mass of the $-Tl(CN)_n$ group with an increasing number of cyano ligands (Table 5).

The NMR spin−spin coupling constants $^1J(^{195}Pt-^{205}Tl)$ show a much more pronounced decreasing trend (Table 5), which, however, reflects mainly a decrease in the s-orbital contribution to the Pt−Tl bonding.[2] Qualitatively, the Pt−Tl σ-bonding molecular orbital can be considered as a result of the symmetry-allowed overlap between the filled platinum $5d_{z^2}$ and the vacant thallium 6s orbital.[2] The thallium 6s valence orbital becomes less available for the platinum d_{z^2} electron pair when the number of strong σ-donor cyano ligands increases and changes the coordination geometry around the thallium atom.

Platinum Coordination. The Pt L_{III}-edge EXAFS data cannot distinguish between the axial and equatorial cyano ligands for the species $[(NC)_5Pt-Tl(CN)_n]^{n-}$ ($n = 1-3$). Therefore, for all samples a mean value was used for the five Pt−C and Pt···N distances, including three- and four-legged multiple-scattering pathways of the same length as Pt···N (cf. Scheme 1). The mean Pt−C and Pt···N distances obtained for the series of dinuclear species are similar, and in all cases the Pt···N distance is about 1.15−1.16 Å longer than Pt−C. The difference is consistent with the expected C−N bond length[27] and with an essentially linear Pt−C−N configuration. The Debye−Waller factors (Pt−C, Pt···N) for the dinuclear complexes are small and close to the corresponding values for the standard compounds (Tables 1 and S1). Thus, the trans effect, i.e., weakening the axial Pt−C bond in a $Pt(CN)_5X$ unit for the above ligands $X = -Tl(CN)_n$, does not increase the $Pt-C_{ax}$ distance enough (>∼0.05 Å) to make it distinguishable by the EXAFS method.

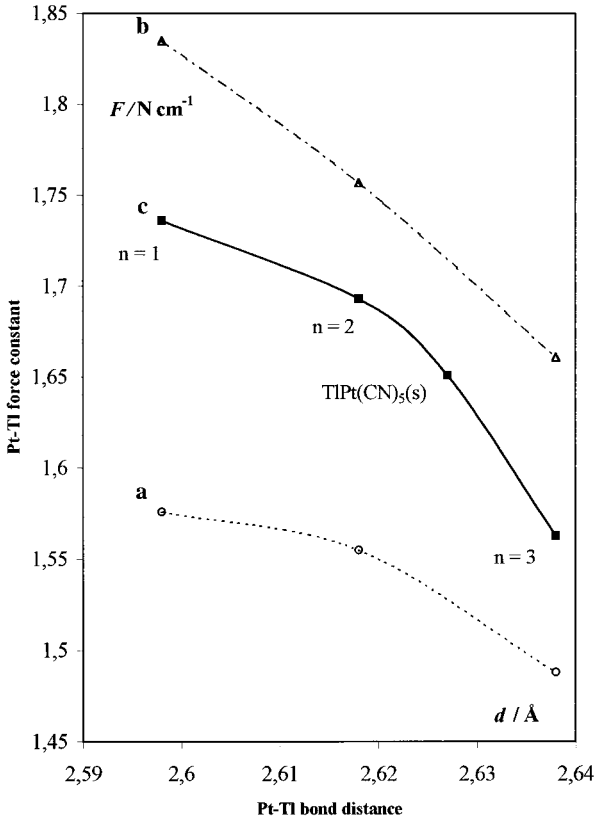

Figure 6. Correlation between Pt−Tl stretching force constants and bond distances: (a) including only the metal atoms; (b) including the axially coordinated cyano ligands; (c) including the full cyano coordination around the metal atoms.

The vibrational spectra give a similar picture. Only a broad asymmetric feature is present in the Pt−C stretching region of the Raman spectra (Figure 4a), which should contain the symmetric (A_1) $Pt-C_{eq}$ breathing mode expected around 470 cm^{-1} (cf. the Supporting Information). Additional information on the platinum coordination environment can be obtained from the C−N stretching region of the dimetallic complexes (Figure 4b,c), in which three Raman and two IR bands can be distinguished by curve-fitting methods (Table 3). The bandwidths are about 8−13 cm^{-1}, with strong overlap. Thus, these bands must contain all four expected fundamental CN stretchings, belonging to the symmetry species $2A_1 + B_1 + E$ of a $(NC)_5Pt-$ group in C_{4v} symmetry.

(25) Shriver, D. F.; Cooper, C. B. In *Vibrational Spectroscopy of Metal−Metal Bonded Transition Metal Compounds*; Shriver, D. F., Cooper, C. B., Eds.; Heyden: London, 1980; Vol. 6, pp 127−157.
(26) Cotton, F. A.; Walton, R. A. *Multiple Bonds Between Metal Atoms*, 2nd ed.; Clarendon Press: Oxford, U.K., 1993.
(27) Golub, A. M.; Köller, H.; Skopenko, V. V. *Chemistry of Pseudohalides*; Elsevier: Amsterdam, 1986.

The two Raman bands appearing at the highest frequencies in the cyanide stretching region of the dimetallic species can be assigned, assuming C_{4v} symmetry of the $(NC)_5Pt-$ group, to the two A_1 (breathing) modes, the intermediate weaker Raman band to the B_1 mode, and the strongest infrared band to the E mode (cf. the Supporting Information).[19] The frequency of the main equatorial A_1 breathing mode decreases slightly: $\nu_1 =$ 2200.1, 2195.6, and 2191.8 cm^{-1} for the three $[(NC)_5Pt-Tl(CN)_n]^{n-}$ complexes with $n = 1-3$, respectively (Table 3). Similar trends were observed for the B_1 modes, $\nu_9 =$ 2189.8, 2183.3, and 2180.5 cm^{-1}, and for the E species, $\nu_{15} =$ 2175.4, 2169.4, and 2165.5 cm^{-1}, for the three complexes, respectively.

A decrease in the C−N frequency of cyano ligands is normally taken as a sign of increased metal to carbon π back-bonding, weakening the C−N bond.[19,21,27,28] The ν_{CN} frequency (2211 cm^{-1}), and the corresponding C−N stretching force constant (Tables 4 and S5), has its highest value for the $[Pt^{IV}(CN)_6]^{2-}$ complex and decreases with an increasing number of cyano ligands on the thallium atom in the $[(NC)_5Pt-Tl(CN)_n]^{n-}$ complexes for $n = 1-3$. The Pt−C force constants, for both the equatorial and axial stretching, decrease abruptly from $[Pt^{IV}(CN)_6]^{2-}$ to the first $[(NC)_5Pt-Tl(CN)_n]^{n-}$ complex ($n = 1$) and are then almost constant for $n = 2$, 3 (Table S5 and Figure S4a). For the $[(NC)_5Pt-Tl(CN)_n]^{n-}$ complexes this reflects the balance between the decreasing Pt−C σ−bond strength and the increasing π-bond strength resulting from the increasing electron density on the platinum atom in this series (cf. Oxidation States of the Metal Atoms). Previously, it was found for the $[Pt(CN)_5X]^{2-}$ (X = Cl, Br, I) complexes that the symmetric equatorial Pt−C and C−N frequencies remain essentially unshifted from those of the parent complex $[Pt^{IV}(CN)_6]^{2-}$ but the apical (trans to X) Pt−C and C−N frequencies shift to lower energies in the order Cl > Br > I.[19]

By means of the previously reported ^{13}C NMR spectra of the aqueous $[(NC)_5Pt-Tl(CN)_n]^{n-}$ species,[2] both the chemical shifts and the platinum−carbon spin−spin coupling constants, $^1J(^{195}Pt-^{13}C)$, are easily obtained for the two types of Pt−C bonds of the $Pt(CN)_5$ unit. The coupling constant for the equatorial carbons, $^1J(^{195}Pt-^{13}C_{eq})$, increases slightly, 820, 821, 832, and 843 Hz, while the axial coupling decreases, $^1J(^{195}Pt-^{13}C_{ax}) =$ 909, 843, 783, and 742 Hz, for $n = 0-3$, respectively, the axial one with a trend similar to that for the $^1J(^{195}Pt-^{205}Tl)$ coupling constant (Table 5). The $^1J(^{195}Pt-^{13}C)$ coupling constant for $[Pt^{IV}(CN)_6]^{2-}$ is 876 Hz. However, the huge two-bond axial thallium−carbon spin−spin coupling, $^2J(^{205}Tl\cdots^{13}C_{ax}) =$ 9743, 8446, and 7270 Hz for $n = 1-3$, respectively, is more than 20 times larger than that for the equatorial carbon atoms, $^2J(^{205}Tl-^{13}C_{eq}) =$ 452, 338, and 255 Hz, respectively.[2] The very large $^2J(^{205}Tl\cdots^{13}C_{ax})$ values imply strong interaction between the thallium atom and the axial cyano ligand within a linear NC−Pt−Tl entity. This can be explained by assuming three-center bonding, involving a combination of the carbon $2p_z$, platinum $5d_{z^2}$, and thallium 6s orbitals under local C_{4v} point group symmetry. Thus, the decreasing trend of the $^1J(^{195}Pt-^{13}C_{ax})$ spin−spin coupling constants observed for the series of Pt−Tl complexes reflects the decreasing s character of the $Pt-C_{ax}$ bond, which is transmitted from the *trans*-Pt−Tl bond, rather than the total strength of the $Pt-C_{ax}$ bond.

Thallium Coordination. Within each $[(NC)_5Pt-Tl(CN)_n]^{n-}$ ($n = 1-3$) species, the cyano ligands coordinated to the thallium atom were found to be equivalent, both from the present Tl L_{III} EXAFS and from the previous NMR data.[2] For comparison, also the mononuclear thallium(III) cyano complexes $[Tl(CN)_{n+1}]^{3-(n+1)}$ ($n = 1-3$)[10] were analyzed here with the current multiple-scattering model based on FEFF calculations (Table 2).

Substitution of one cyano ligand in *trans*-$[Tl(CN)_2(H_2O)_4]^+$ by a $Pt(CN)_5$ group gives the complex $[(NC)_5Pt-Tl(CN)(H_2O)_4]^-$. The Tl−C and Tl···N distances (2.128(4) and 3.284(6) Å, respectively) are both longer in the dimetallic complex than in the mononuclear one (2.092(4) and 3.263(3) Å, respectively) but are in both cases consistent with linear Tl−C−N coordination (Table 2). As in the parent *trans*-$[Tl(CN)_2(H_2O)_4]^+$ species, we assume that the coordination environment of the thallium atom in a hydrated $[(NC)_5Pt-Tl(CN)(H_2O)_4]^-$ species is pseudo-octahedral with four weakly coordinated equatorial water molecules. However, the short Tl−Pt distance to the bulky $Pt(CN)_5$ group may cause some steric interaction, as indicated in Figure 5a. The Tl−O bonds are longer in the dimetallic species (about 2.51 Å) than in the mononuclear complex (2.43 Å) (Table 2).

Also for the $[(NC)_5Pt-Tl(CN)_2]^{2-}$ and $[(NC)_5Pt-Tl(CN)_3]^{3-}$ complexes, the Tl−C and Tl−N distances increase significantly but are still consistent with linear Tl−C−N bonding (Table 2). The Tl−C bond length increases to 2.22 Å (see below) for the $[(NC)_5Pt-Tl(CN)_3]^{3-}$ species (Figure 5b), which indicates a change to tetrahedral coordination geometry, as in the related $[Tl(CN)_4]^-$ complex.[10] A trigonal coordination geometry of the thallium atom seems likely for the $[(NC)_5Pt-Tl(CN)_2]^{2-}$ species, similar to that for the halide complexes $[TlX_3(H_2O)_2]$ (X = Cl, Br).[10] Possibly there is also weak hydration of the thallium atom as in the halide species, even though no Tl−O interaction could be detected in the EXAFS data.

The mean Tl−C distance (2.206(6) Å), obtained for the solution where $[(NC)_5Pt-Tl(CN)_2]^{2-}$ was the dominating species (Table 2), appears surprisingly long, considering that in the hydrated mononuclear $[Tl(CN)_3(H_2O)]$ complex the Tl−C distance is 2.133(4) Å, intermediate between those of the $[Tl(CN)_2(H_2O)_4]^+$ and $[Tl(CN)_4]^-$ complexes (2.092(4) and 2.176(6) Å, respectively). However, these mean values for both the $[(NC)_5Pt-Tl(CN)_2]^{2-}$ and $[(NC)_5Pt-Tl(CN)_3]^{3-}$ complexes are affected by the presence of additional complexes in solution.[8] In both cases the dominating $[(NC)_5Pt-Tl(CN)_n]^{n-}$ complex contained less than 75% of the total thallium concentration at the equilibrium composition. For $[(NC)_5Pt-Tl(CN)_2]^{2-}$, the remainder consists of equal amounts of the species $[(NC)_5Pt-Tl(CN)(H_2O)_4]^-$, with one Tl−C distance, and $[(NC)_5Pt-Tl(CN)_3]^{3-}$, with three Tl−C distances. In the $[(NC)_5Pt-Tl(CN)_3]^{3-}$ solution there is 25% $[Tl(CN)_4]^-$ present with four shorter Tl−C distances. Thus, the extra Tl−C distances should *increase* the mean value obtained for the Tl−C bond distances for the $[(NC)_5Pt-Tl(CN)_2]^{2-}$ solution, while a *decrease* is expected for the $[(NC)_5Pt-Tl(CN)_3]^{3-}$ solution. The Tl−C bond distances of the $[(NC)_5Pt-Tl(CN)_2]^{2-}$ species, corrected for the presence of other species with different numbers of Tl−C distances, can be estimated as 2.20(2) Å and for the $[(NC)_5Pt-Tl(CN)_3]^{3-}$ complex as 2.22(2) Å.

In the vibrational spectra several broad bands were observed in the frequency range expected for Tl−O and Tl−C bond stretching (325−400 cm^{-1}; cf. Figure 4a). Assignments were made of the symmetric and asymmetric Tl−C stretching modes for the $-Tl(CN)_n$ groups on the basis of a previous investigation (cf. the Supporting Information).[10] The resulting force constants (Table S5) are consistent with the weakening of the Tl−C bonds, which is expected from the increasing bond distance and the

(28) Nakamoto, K. *Infrared and Raman Spectra of Inorganic and Coordination Compounds*; 5th ed.; Wiley-Interscience: New York, 1997; Part B, Chapter III-15.

increased electron transfer from the thallium to the platinum atom with increasing number of cyano ligands (see Oxidation States of the Metal Atoms). In the cyanide stretching region we assign the broad Raman band at the lowest frequency, 2178, 2168, and 2161 cm^{-1}, with increasing intensity for $n = 1-3$, respectively, to the cyano ligands of the thallium atom (Figure 4b and Table 3). The symmetric stretching vibrations of the corresponding mononuclear $[Tl^{III}(CN)_{n+1}]^{3-(n+1)}$ complexes appear at higher wavenumbers: 2187, 2187, and 2180 cm^{-1}, respectively.[10]

Another sensor of the Tl−C bond character is the one-bond spin−spin coupling constant $^1J(^{205}Tl-^{13}C)$, which decreases dramatically for the $[(NC)_5Pt-Tl(CN)_n]^{n-}$ species: 2446, 876, and 52 Hz for $n = 1-3$, respectively.[2] This decrease can be attributed to the decreasing s character of the Tl−C bonds, which is influenced by the thallium coordination geometry. The metal−metal bonding also has a strong influence on the thallium−carbon coupling and the s character of the bonds, as shown by the substantially larger values of $^1J(^{205}Tl-^{13}C)$ for the corresponding $[Tl^{III}(CN)_{n+1}]^{3-(n+1)}$ species: 13 749, 7954, and 5436 Hz.[9]

Oxidation States of the Metal Atoms. The chemical shifts of both the ^{195}Pt and ^{205}Tl nuclei are quite sensitive to changes in the oxidation state of the metal ions.[29−31] The shifts in the series of dinuclear complexes $[(NC)_5Pt-Tl(CN)_n]^{n-}$ fall in the wide interval between the characteristic aqueous solution values for complexes with the metal atoms in their two limiting oxidation states: e.g. for platinum, Pt^{IV} in $[Pt(CN)_6]^{2-}$ and Pt^{II} in $[Pt(CN)_4]^{2-}$; for thallium, Tl^I in Tl^+_{aq} and Tl^{III} in $[Tl(CN)_4]^-$ (see Table 5).[2,9]

When additional cyano ligands coordinate to the thallium atom in the dinuclear complexes, the chemical shifts of the metal atoms gradually change with opposite trends for δ_{Pt} and δ_{Tl} (Table 5 and Figure S6). Thus, the decreasing shielding of the thallium nucleus is coupled to an increase in the shielding of the platinum nucleus, which implies a transfer of electron density from thallium to platinum when the number of cyano ligands increases. With the chemical shifts for the above complexes, $[Pt^{IV}(CN)_6]^{2-}$, $[Pt^{II}(CN)_4]^{2-}$ and Tl^+_{aq}, $[Tl^{III}(CN)_4]^-$, as reference values, the δ_{Pt} and δ_{Tl} values in the series of dinuclear species $[(NC)_5Pt-Tl(CN)_n]^{n-}$ ($n = 0-3$) can be used to estimate the relative amount of electron transfer between the metal atoms. With the use of the integer oxidation states for the complexes above as starting points, this electron transfer can be expressed in terms of "relative oxidation states" in a linear interpolation. The values vary for platinum from 3.6 to 2.6 and for thallium from 1.5 to 2.5, respectively, when n increases from 1 to 3 (cf. Table 5 and ref 32).

This "relative oxidation state" increases for the thallium atom and decreases for platinum, with the sum close to the expected value of 5, when the number of cyano ligands increases in the series of complexes. Thus, the increased negative charge of the $-Tl(CN)_n$ group seems to be partly transferred from the thallium to the platinum atom via the Pt−Tl bond. The values obtained for the $[(NC)_5Pt-Tl(H_2O)_x]$ complex indicate that the electron pair of the σ bond is located more in the thallium 6s than in the platinum d_{z^2} orbital. Also for the solid $(NC)_5Pt-Tl$ compound intermediate relative oxidation states could be derived for the metal atoms, in this case from X-ray photoelectron spectra.[5] The obtained values, $Pt^{3.2}/Tl^{1.6}$, are similar to those for the complex $[(NC)_5Pt-Tl(H_2O)_x]$ in solution, $Pt^{3.6}/Tl^{1.5}$.

This gradual charge transfer indicated by the NMR chemical shifts is also supported by preliminary results from ab initio calculations on the charge distribution in the $[(NC)_5Pt-Tl(CN)_n]^{n-}$ complexes.[33] The Mulliken charge for thallium increases stepwise, +0.19 and +0.06 e, with a corresponding decrease for platinum, −0.27 and −0.12 e, when the number of cyano ligands increases from $n = 1$ to 2 and from $n = 2$ to 3, respectively.

To summarize, when the cyanide ions bind to the thallium atom, two effects seem to occur: (1) an increase in the transfer of the bonding electron pair toward platinum and (2) an increase in the electron density on thallium from the cyano ligands. The former effect is consistent with an increase in the Pt−Tl bond distance.

Correlation with Vibrational Spectra. Attempts have previously been made to correlate shifts in the vibrational frequencies of cyano groups to, for example, the Pt oxidation state in partially oxidized tetracyanoplatinate one-dimensional conductors, since the cyanide stretching mode should be particularly sensitive to the electron density of the platinum atom.[34] Stretching frequencies of cyano ligands usually increase with an increasing charge on the metal atom.[28] The reason for this is rather complex and can for transition metals be considered to originate from a combination of two effects: (1) a strong σ-bond withdrawing negative charge from the cyano carbon atom (from the nonbonding 2σ electron pair) and thus resulting in a stronger C−N bond and (2) decreased availability of the filled metal d orbitals, which can back-bond to the cyano $\pi^*(2p)$ antibonding orbital and weaken the C−N bond.[21,27,35,36] Thus, for the $[Pt^{IV}(CN)_6]^{2-}$ complex the Raman-active C−N symmetric stretching (A_{1g}) frequency becomes very high, 2211 cm^{-1}. For $[Pt^{II}(CN)_4]^{2-}$ the corresponding A_{1g} mode is found at 2168 cm^{-1}, consistent with an increased Pt→CN π^* back-bonding because of higher availability of the platinum d electrons for the lower oxidation state.[22] For partially oxidized tetracyanoplatinate compounds the corresponding C−N stretching frequency is intermediate: e.g. 2182 cm^{-1} for $K_2[Pt^{II}(CN)_4]Br_{0.33}$.[34]

A similar situation is found for the $(NC)_5Pt-$ unit of the dinuclear $[(NC)_5Pt-Tl(CN)_n]^{n-}$ ($n = 1-3$) complexes, where the A_1 equatorial and axial stretching frequencies (Tables 3 and S4) occur between the corresponding values of Pt^{II} and Pt^{IV} cyano complexes. The bands shift to lower frequency with an increasing number of cyano ligands in the complexes. Also, the IR-active E mode stretching frequency of the $(NC)_5Pt$ entity falls between the T_{1g} vibration of $[Pt^{IV}(CN)_6]^{2-}$ (2191 cm^{-1})[27] and the E_u mode of $[Pt^{II}(CN)_4]^{2-}$ (2133 cm^{-1}) (cf. Figure 4c and Table S4). The C−N bond stretching force constants have been evaluated by normal-coordinate analyses (Tables 4 and S5). They decrease for both the equatorial and axial cyano ligands of the $(NC)_5Pt-$ unit, when the number of cyano ligands

(29) Glaser, J. In *Advances in Inorganic Chemistry*; Sykes, A. G., Ed.; Academic Press: San Diego, CA, 1995; Vol. 43, pp 1−78.
(30) Hinton, J. F.; Metz, K. R.; Briggs, R. W. *Prog. Nucl. Magn. Reson. Spectrosc.* **1988**, *20*, 423−513.
(31) Pregosin, P. S. *Transition Metal Nuclear Magnetic Resonance*; Elsevier: Amsterdam, 1991; Vol. 13.
(32) Maliarik, M. Ph.D. Thesis, The Royal Institute of Technology, Stockholm, Sweden, 2001.
(33) Kloo, L.; Glaser, J.; Maliarik, M. unpublished results. Computation level: restricted HF, SDD basis set ((8s7p6d)/[6s5p3d] and (4s4p1d)/[2s2p1d] for platinum and thallium, respectively), MWB (effective core potential) 60 and 78 for platinum and thallium, respectively.
(34) Ferraro, J. R.; Basile, L. J.; Williams, J. M.; McOmber, J. I.; Shriver, D. F.; Greig, D. R. *J. Chem. Phys.* **1978**, *69*, 3871.
(35) Dunbar, K. R.; Heintz, R. A. In *Chemistry of Transition Metal Cyanide Compounds: Modern Perspectives*; Dunbar, K. R., Heintz, R. A., Eds.; Wiley: New York, 1997; Vol. 45, pp 283−391.
(36) Sharpe, A. G. *Cyanides and Fulminates*; Sharpe, A. G., Ed.; Pergamon Press: Oxford, U.K., 1987; Vol. 2, pp 7−14.

increases on thallium: i.e., for a decreasing charge on the platinum atom (Table 4 and Figure S4b).

For the mononuclear complexes $[Tl(CN)_{n+1}]^{3-(n+1)}$ with $n = 0-3$, both the Tl−C and C−N stretching force constants decrease monotonically (Table 4 and Figure S5). Replacing one cyano ligand with a $(NC)_5Pt-$ unit to form the dinuclear complexes $[(NC)_5Pt-Tl(CN)_n]^{n-}$ ($n = 1-3$) shifts both the Tl−C and the C−N symmetric stretching vibrations to lower frequencies. Also, the corresponding Tl−C distances increase (Table 2), showing that the Tl−C bond is weaker in the dimetallic compounds. However, in the $[(NC)_5Pt-Tl(CN)_n]^{n-}$ ($n = 1-3$) series, the C−N force constant has its smallest value for the intermediate complex, $[(NC)_5Pt-Tl(CN)_2]^{2-}$, indicating an increase in the back-bonding from the thallium atom. The increase in the Tl−C distance, about 0.07 Å from that in the probably tetrahedral $[Tl(CN)_3(OH_2)]$ complex, also seems to be largest for this complex and suggests a different coordination geometry with more than one water molecule hydrating the thallium atom.

Even though the axial Pt−C stretching force constants are much smaller than the equatorial ones (Figure S4, Table 4), both sets show some *increase*, despite the decreasing charge on platinum, for the dimetallic complexes with $n = 1-3$, respectively. Moreover, despite the corresponding increasing "relative oxidation state" on the thallium atom, the Tl−C stretching force constant decreases. This shows that no simple correlation between metal atom charge and bond strength, as estimated from force constants and vibrational spectra, can be made for the delocalized bonds in this series of dimetallic complexes.

Platinum−Thallium Bond Distances. As discussed above, the short platinum−thallium bond length for the $[(NC)_5Pt-Tl(CN)_n]^{n-}$ complexes increases for $n = 1-3$: 2.60(1), 2.62(1), and 2.64(1) Å, respectively (Table 5). These metal−metal distances can be compared with bond lengths of $Pt^{III}-Pt^{III}$ and $Tl^{II}-Tl^{II}$ in homodinuclear compounds, with the metal atoms in oxidation states close to those in the present complexes. A recent structural study of a dimeric complex of trivalent platinum, $[(NC)_5Pt-Pt(CN)_5]^{4-}$, gives a direct unsupported $Pt^{III}-Pt^{III}$ bond length in aqueous solution of 2.73 Å.[37] No similar complex with thallium(II) has been found. However, a comparison can be made with the Tl−Tl bond distance 2.91 Å from the structure of tetrakis(hypersilyl)dithallium(II).[38] Thus, the Pt−Tl distances in the $[(NC)_5Pt-Tl(CN)_n]^{n-}$ ($n = 1-3$) species are significantly shorter than the mean of these two distances, 2.82 Å, indicating strong covalency in the Pt−Tl bond.

Usón et al. recently reported the structure of a number of dimetallic compounds with direct $Pt^{II}-Tl^{I}$ contacts.[39] They concluded that an increasing donor strength character of the platinum atom reduces the Pt−Tl distance. However, in the present case the donor property of the platinum center in the $(NC)_5Pt-$ group should be virtually constant in the series of $[(NC)_5Pt-Tl(CN)_n]^{n-}$ complexes. The shortening of the metal−metal bond when reducing the number of cyano ligands from 3 to 1 is due, rather, to an increase in acceptor character of the thallium atom.

In an overview of Pt−Tl distances for structurally characterized compounds three groups can be distinguished, which depend on the formal oxidation state of the metal atoms: $Tl^{I}-Pt^{0}$ (2.79−3.05 Å),[40−42] $Tl^{I}-Pt^{II}$ (2.88−3.14 Å),[39,43−48] and $Tl^{II}-Pt^{II}$ (2.70−2.71 Å).[49] The bond distances in the presently studied complexes are shorter, $[(NC)_5Pt-Tl(CN)_n]^{n}$ ($n = 1-3$) (2.60−2.64 Å), as is also the case for a number of related solid compounds which recently have been structurally characterized in this laboratory: $[TlPt(CN)_5]$ (2.63 Å),[5] $[(NC)_5Pt-Tl(dmso)_4]$ (2.61 Å),[50] $[(NC)_5Pt-Tl(en)_2]$ (2.64 Å),[50] $[(NC)_5Pt-Tl(bipy)(dmso)_3]$ (2.62 Å),[51] $[(NC)_5Pt-Tl(bipy)_2]$ (2.61 Å),[51] and $[(NC)_5Pt-Tl(H_2O)(nta)]^{3-}$ (2.61 Å).[32] Even though the electron transfer between the two metal atoms may vary, the short platinum−thallium distance is consistent with the higher total oxidation state (V) of the two metal atoms.

Conclusions

This work finalizes the structural characterization of the family of dinuclear $[(NC)_5Pt-Tl(CN)_n]^{n-}$ complexes initiated in this laboratory.[1,2] The platinum−thallium and metal−ligand distances have been determined in aqueous solutions of the complexes $[(NC)_5Pt-Tl(CN)_n]^{n-}$ ($n = 1-3$) by means of the EXAFS technique. The short Pt−Tl distancse, 2.60(1), 2.62(1), and 2.64(1) Å, which increase for $n = 1-3$, respectively, confirm the previous conclusion of a nonsupported direct metal−metal bond. Also, the values of the force constant of the Pt−Tl bond, which have been obtained by normal-coordinate analyses of vibrational spectra, are characteristic for single metal−metal bonds. They show the same trend, namely weakening of the metal−metal bond with coordination of additional cyano ligands to the thallium atom. This is also consistent with our previous spectroscopic characterization of these species, e.g. the trend of the spin−spin coupling constants $^1J(^{195}Pt-^{205}Tl)$.

The structure of the pentacyanoplatinum group shows only a minor change in the current series of dimetallic complexes. The EXAFS data could only give a mean Pt−C distance of 2.00−2.01 Å for the five cyano ligands of the platinum atom. Also, the stretching force constants indicate relatively small changes in the bond strength. However, the drastic changes in the thallium coordination geometry and bonding cause variations in the characteristic properties, including the change in the Pt−Tl distances. In the $[(NC)_5Pt-Tl(CN)_3]^{3-}$ complex the thallium atom is probably tetrahedrally four-coordinated with three Tl−C bonds of 2.22(2) Å, while two strong Tl−C bonds of 2.20(2) Å are formed in the intermediate complex $[(NC)_5Pt-Tl(CN)_2]^{2-}$, possibly with additional weak coordination of water molecules. The thallium atom coordinates one cyano ligand in the hydrated $[(NC)_5Pt-Tl(CN)(H_2O)_4]^{-}$ complex in a linear NC−Pt−Tl−CN entity, with the Tl−C bond distance of 2.13(1) Å and probably four water molecules loosely bound to thallium with a mean Tl−O distance of about 2.51 Å.

When one cyano ligand of the mononuclear $[Tl(CN)_{n+1}]^{3-(n+1)}$ complexes is replaced by a $(NC)_5Pt-$ group, forming $[(NC)_5Pt-$

(37) Jalilehvand, F.; Ilyuhin, A.; Glaser, J.; Maliarik, M.; Sandström, M.; Tóth, I. Unpublished results.
(38) Henkel, S.; Klinkhammer, K. W.; Schwarz, W. *Angew. Chem., Int. Ed. Engl.* **1994**, *33*, 681.
(39) Usón, R.; Fornies, J.; Tomas, M.; Garde, R.; Merino, R. I. *Inorg. Chem.* **1997**, *36*, 1383.
(40) Ezomo, O. J.; Mingos, M. P.; Williams, I. D. *J. Chem. Soc., Chem. Commun.* **1987**, 924.
(41) Hao, L.; Vittal, J. J.; Puddephatt, R. J. *Inorg. Chem.* **1996**, *35*, 269.
(42) Catalano, V. J.; Bennett, B. L.; Yson, R. L.; Noll, B. C. *J. Am. Chem. Soc.* **2000**, *122*, 10056.
(43) Nagle, J. K.; Balch, A. L.; Olmstead, M. M. *J. Am. Chem. Soc.* **1988**, *110*, 319.
(44) Balch, A.; Rowley, S. P. *J. Am. Chem. Soc.* **1990**, *112*, 6139.
(45) Renn, O.; Lippert, B. *Inorg. Chim. Acta* **1993**, *208*, 219.
(46) Klepp, K. O. *J. Alloys Compd.* **1993**, *196*, 25.
(47) Bronger, W.; Bonsmann, B. *Z. Anorg. Allg. Chem.* **1995**, *621*, 2083.
(48) Ara, I.; Berenguer, J. R.; Fornies, J.; Gomez, J.; Lalinde, E.; Merino, R. I. *Inorg. Chem.* **1997**, *36*, 6461.
(49) Usón, R.; Fornies, J.; Tomas, M.; Garde, R.; Alonso, P. *J. Am. Chem. Soc.* **1995**, *117*, 1837.
(50) Ma, G.; Kritikos, M.; Glaser, J. *Eur. J. Inorg. Chem.* **2001**, 1311.
(51) Ma, G.; Kritikos, M.; Maliarik, M.; Glaser, J. Submitted for publication.

$Tl(CN)_n]^{n-}$ ($n = 1-3$) complexes, the Tl−C distances increase by about 0.04−0.07 Å, consistent with smaller Tl−C force constants in the dinuclear species, and charge transfer occurs from thallium via the Pt−Tl bond, as indicated by the NMR chemical shifts. The electron transfer between the metal atoms in the current series of dimetallic Pt−Tl complexes is discussed in terms of "relative oxidation states" of the metal atoms. These were evaluated by means of the ^{195}Pt and ^{205}Tl NMR chemical shifts, intermediate for platinum between Pt^{II} in $[Pt(CN)_4]^{2-}$ and Pt^{IV} in $[Pt(CN)_6]^{2-}$, and for thallium between Tl^{I} in the hydrated Tl^{+}_{aq} ion and Tl^{III} in $[Tl(CN)_4]^{-}$. The obtained values indicate a gradual charge transfer from the thallium cyano entity to platinum when additional negative cyanide ions coordinate to thallium. The complexes can be considered as metastable intermediates in a two-electron-transfer process between Pt^{II} and Tl^{III} cyano complexes, where the final products of the redox reaction are Pt^{IV} and Tl^{I} species.[3,4]

Acknowledgment. We wish to acknowledge the financial support of the Swedish Research Council, the European Commission INTAS Program, the Russian Foundation for Fundamental Research (Grant No. RFFI 98-03-32651), the Carl Trygger Foundation for Scientific Research, the Wenner-Gren Center Foundation, and the Hungarian National Scientific Research Foundation (Grant Nos. OTKA T026115 and T025278). We gratefully acknowledge the Stanford Synchrotron Radiation Laboratory (SSRL) for allocation of beam time and laboratory facilities. The SSRL is operated by the Department of Energy, Office of Basic Energy Sciences. The SSRL Biotechnology Program is supported by the National Institutes of Health, National Center for Research Resources, Biomedical Technology Program, and by the Department of Energy, Office of Biological and Environmental Research.

Note Added in Proof. The special nature and properties of the currently investigated species have already inspired two computational studies. One is dealing with the geometric structure of the $[(NC)_5PtTl(CN)_n]^{n-}$, $n = 0$, 1, 2, or 3, species,[52] and the other with the nuclear spin−spin coupling in the $[(NC)_5PtTl(CN)]^{-}$ complex.[53] Both studies give results in reasonable agreement with the experimentally derived structures and confirm that the hydration of the thallium atom is important for the properties, especially for the remarkable spin−spin coupling pattern found from our previous NMR data. The difference in the calculated Pt−C bond distances for axial and equatorial ligands is small, consistent with the EXAFS results. The calculated Tl−O bond distance for a $[(NC)_5PtTl(CN)(H_2O)_4]^{-}$ species is 2.54 Å,[53] in good agreement with the experimental value 2.51(1) Å.

Supporting Information Available: Results of analyses of Pt L_{III} and Tl L_{III} edge EXAFS data (Tables S1−S3), an appendix giving a detailed account of the assignment of the vibrational spectra, on the basis of calculated frequencies and comparisons with previous assignments of related complexes, assignments and normal-coordinate analyses of vibrational spectra of $[Pt(CN)_6]^{2-}$ and $[(NC)_5Pt-Tl(CN)_n]^{n-}$ complexes $n = 1-3$) (Tables S4 and S5), Pt L_{III} EXAFS filtered functions for the solid reference compounds $K_2[Pt^{II}(CN)_4]\cdot 3H_2O$ and $K_2[Pt(CN)_6]$, together with the model fits and corresponding Fourier transforms (Figures S1 and S2), a description of internal coordinates used for force constant calculations (Figure S3), Pt−C, Tl−C, and C−N force constants for the cyano ligands of $[Pt(CN)_6]^{2-}$ and the solution complexes $[Tl(CN)_{n+1}]^{3-(n+1)}$ and $[(NC)_5Pt-Tl(CN)_n]^{n-}$ ($n = 1-3$) (Figures S4 and S5), NMR ^{195}Pt and ^{205}Tl chemical shifts of the dinuclear species $[(NC)_5Pt-Tl(CN)_n]^{n-}$ ($n = 1-3$), in aqueous solution, as a function of the number of cyano ligands n of the thallium atom (δ_{Pt},circles; δ_{Tl}, dots) (Figure S6), and Raman spectrum of $[(NC)_5Pt-Tl(CN)(H_2O)_4]^{-}$ in aqueous solution in the range 400−500 cm^{-1} (Figure S7; the insets show the observed spectral ranges for fundamentals of solid $M_2[Pt(CN)_5X]$ compounds, where M = Na, K, Cs and X = Cl, Br, I[19]). This material is available free of charge via the Internet at http://pubs.acs.org.

IC010055H

(52) Russo, M. R.; Kaltsoyannis, N. *Inorg. Chim. Acta* **2001**, *312*, 221.
(53) Autschbach, J.; Ziegler, T. *J. Am. Chem. Soc.* **2001**, *123*, 5320.